An Algorithm for Distorted Fingerprint Matching Based on Local Triangle Feature Set

Xinjian Chen, Jie Tian, *Senior Member, IEEE*, Xin Yang, and Yangyang Zhang

Abstract—Coping with nonlinear distortions in fingerprint matching is a challenging task. This paper proposes a novel method, a fuzzy feature match (FFM) based on a local triangle feature set to match the deformed fingerprints. The fingerprint is represented by the fuzzy feature set: the local triangle feature set. The similarity between the fuzzy feature set is used to characterize the similarity between fingerprints. A fuzzy similarity measure for two triangles is introduced and extended to construct a similarity vector including the triangle-level similarities for all triangles in two fingerprints. Accordingly, a similarity vector pair is defined to illustrate the similarities between two fingerprints. The FFM method maps the similarity vector pair to a normalized value which quantifies the overall image to image similarity. The proposed algorithm has been evaluated with NIST 24 and FVC2004 fingerprint databases. Experimental results confirm that the proposed FFM based on the local triangle feature set is a reliable and effective algorithm for fingerprint matching with nonlinear distortions.

Index Terms—Distortion, fingerprint recognition, matching, minutia, similarity measure.

I. INTRODUCTION

FINGERPRINT recognition has been applied to identify criminals in law enforcement, and currently it is being increasingly used for personal identification in a civilian's daily life, such as an ID card, fingerprints hard disk, and so on. Various fingerprint recognition techniques, including fingerprint acquisition, enhancement, matching, and classification are developed and advanced rapidly. However, there are still difficult and challenging tasks in this field. One of the main difficulties in matching two fingerprint impressions of the same finger is to deal with the nonlinear distortions, which are caused by the acquisition process. When capturing, the three-dimensional (3-D) elastic surface of a finger is pressed onto a flat sensor surface, and this 3-D–two-dimensional (2-D) mapping introduces nonlinear distortions, especially if the force is not

Fig. 1. Example of large distortion from FVC2004 DB1. (a) 102_3.tif, (b) 102_5.tif, and (c) the map relations of the corresponding minutiae in fingerprint images 102_3 and 102_5, (d) the image is fingerprint 102_5 (after registration) added to 102_3. In the rectangle region, the corresponding minutiae are approximately overlapped. While in the ellipse region, the maximal vertical difference of corresponding minutiae is more than 100 pixels.

orthogonally applied to the sensor [1]. The distortion is associated with several reasons [2], including the sensor orientation with the finger, the applied pressure, the disposition of the subject, the motion of the finger prior to its placement on the sensor, the skin moisture, and the elasticity of the skin, etc. It is a realistic situation for noncooperative users who deliberately apply excessive force to create intentional elastic deformations. In Fingerprint Verification Competition 2004 (FVC2004) [3], individuals were requested to exaggerate the skin distortion during the certain fingerprint capturing process. Fig. 1 shows a pair of fingerprints of large distortion from FVC2004 DB1 (102_3.tif and 102_5.tif). While the corresponding minutiae in the rectangle region are approximately overlapped, the maximal distance between corresponding minutiae in the ellipse region is more than 100 pixels. In order to improve the whole fingerprint recognition system, these nonlinear distortions must be well accounted for.

There are different attempts to deal with the nonlinear distortions in fingerprint images. These include the methods based on detecting the distortion [4]–[6]; bounding box [7]–[9]; local similarity [10]–[13]; deformation model [1], [2], [14]; and others [15], [16].

Some methods measured the forces and torques on the scanner directly with the aid of specialized hardware [4], or detected and estimated the distortion occurring in fingerprint videos [5]. If excessive force is applied or the estimated distortion is too large, the captured fingerprint image will be deleted. However, these methods do not work with the collected images. Chen *et al.* [6] computed the registration pattern (RP) between two fingerprints which inspects whether it is within a genuine RP space. If it is, further fine matching will be conducted.

In some methods, a bounding box was used to match the deformed fingerprints [7]–[9]. In Jain's algorithm [7], a fixed-size

bounding box was used during the matching process. Luo *et al.* [8] improved this algorithm, a changeable bounding box had been applied during the matching process which made it more robust to nonlinear deformations between the images. Lee *et al.* [9] addressed a minutiae-based fingerprints matching algorithm by using distance normalization and local alignment to deal with the nonlinear distortion. However, in order to tolerate the position change of the corresponding minutiae because of plastic distortions, the size of the bounding boxes had to be increased. As a side effect, this may lead to a higher false acceptance rate by wrongly pairing the nonmatching minutiae.

Some of the matching techniques computed the local similarity to improve the robustness of the distortion affecting fingerprint patterns since the local similarity was less affected by plastic distortions [10]–[13]. Ratha *et al.* [10] used the local neighborhood structures to get the corresponding minutiae pairs. Kovács–Vajna *et al.* [11] proposed a triangular matching method to cope with the strong deformation of fingerprint images, which graphically demonstrated that the large cumulative effects can result from small local distortions. Jiang *et al.* [12] addressed a method which relies on a similarity measure defined between local structural feature to align two patterns and calculate a matching score between the two minutiae lists. Wahab *et al.* [13] developed a method using groups of minutiae to define a local structural feature. The matching is based on the pairs of corresponding structural features which are identified between two fingerprint impressions. These methods only solve part of the nonlinear deformations.

Some researchers proposed the deformation models to describe the nonlinear distortions in fingerprint images [1], [2], [14]. Maio *et al.* [14] proposed a plastic distortion model to cope with the nonlinear deformations. In this method, the physical cause of the distortion is modeled by distinguishing three distinct concentric regions in a fingerprint. Experiments have shown that this model provides an accurate description of the plastic distortions, but it is difficult to accurately estimate the distortion parameters. Bazen *et al.* [1] employed a thin-plate spline model to describe the nonlinear distortions between two sets of possible matching minutiae pairs. They use a thin-plate spline (TPS) model to align every pair of impressions, even if they are from two different fingers. It forces an alignment between impressions originating from two different fingers and, therefore, results in a higher false accept rate. Ross *et al.* [2] improved Bazen's method [1], using the average deformation computed from the fingerprint impressions of the same finger based on the thin-plate spline model to cope with the nonlinear distortions.

There are other methods proposed to deal with the distortion [15], [16]. Senior *et al.* [15] proposed an algorithm that first estimated the local ridge frequency in the entire fingerprint and then converted a distorted fingerprint image into an equally ridge spaced fingerprint. Although the stricter matching condition slightly increases the algorithm performance, this method only solves a part of the nonlinear deformations. Chen *et al.* [16] proposed an algorithm based on fuzzy theory to deal with the nonlinear distortion. In this algorithm, the local topological structure matching was introduced to improve the robustness of global alignment. A method based on fuzzy theory, normalized

fuzzy similarity measure was conducted to compute the similarity between the template and input fingerprints.

Different from the above mentioned methods, we developed a novel way, fuzzy feature match (FFM) based on a local triangle feature set to match the deformed fingerprints. The fingerprint was represented by the fuzzy feature set: local triangle feature set. The similarity between the fuzzy feature set was used to characterize the similarity between fingerprints. A fuzzy similarity measure for two triangles was first introduced. The result was then extended to construct a similarity vector which includes the triangle-level similarities for all triangles in two fingerprints. Accordingly, a similarity vector pair was defined to illustrate the similarities between two fingerprints. Finally, the FFM measure mapped a similarity vector pair to a normalized quantity within the real interval [0, 1], which quantifies the overall image to image similarity. The proposed algorithm was evaluated with NIST 24 and FVC2004 fingerprint databases. Experimental results indicate that our algorithm works well with the nonlinear distortions. For deformed fingerprints, the algorithm gives considerably higher matching scores compared to conventional matching methods. The equal error rate (EER) of the proposed algorithm on NIST 24 is about 3.11%. In the fingerprint database, DB1 and DB3 of FVC2004, EER are 4.06% and 1.35%, respectively, although there is a large distortion between some fingerprints from the same finger.

The rest of this paper is organized as follows. Section II explains the fingerprint preprocessing and minutiae extraction process. Section III presents the detail of the novel method, FFM, based on the local triangle feature set for deformed fingerprints matching. Section IV gives out the theoretical analysis of the method. The performance of our algorithm is shown by experiments in Section V. Section VI is the conclusion.

II. FINGERPRINT PREPROCESSING AND MINUTIAE EXTRACTION

The method proposed by Hong *et al.* [17] is used to enhance the image and obtain the thinned ridge map. The thinned ridge map is postprocessed by Luo's method [18]. Then, the minutiae sets M are detected by Hong's method [17].

It is difficult to reliably extract minutiae from the input fingerprint, especially from the low-quality fingerprints. The performance of the minutiae extraction algorithm highly depends on the quality of the input images. However, in reality, about 10% [17] of acquired fingerprints are of poor quality due to variations in impression or skin condition, ridge configuration, acquisition devices, and noncooperative attitude of subjects, etc. For those poor images, some spurious minutiae may exist even after fingerprint enhancement and postprocessing. It is necessary to develop an algorithm to work with these spurious minutiae.

A method proposed in our previous work [16] is used to judge whether an extracted minutiae is a true one. According to our experience, the distance between true minutiae is generally greater than a certain value. While near the spurious minutiae, there are usually other spurious minutiae, and they are often detected at the border of the fingerprint image. The detailed algorithm for dealing with the spurious minutiae is described in another paper [16]. None of the detected spurious minutiae are included in the further matching process.
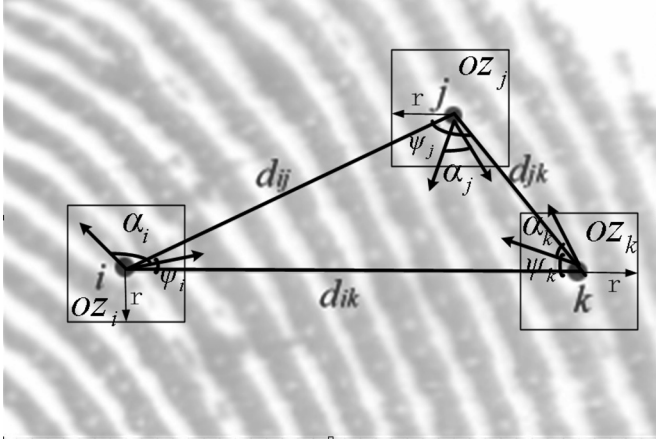
Fig. 2. Local triangle structure of the fingerprint.

Fig. 3. Genuine distorted pattern derived from a true matching attempt. (a) Template image. (b) Input image. (c) Genuine distorted pattern.

III. FUZZY FEATURE REPRESENTATION AND FUZZY MATCH

A. Defining Local Triangle Feature Set

In our algorithm, the block of the matching is the local triangle feature of the fingerprints. The feature vector of a local triangle structure T_k is defined as $FT_k = \{d_{ij}, d_{ik}, d_{jk}, \psi_i, \psi_j, \psi_k, OZ_i, OZ_j, OZ_k, \alpha_i, \alpha_j, \alpha_k\}$ where d_{ij} denotes the distance between minutiae i and j; and ψ_i indicates the angle between the direction from minutiae i to j and the direction from minutiae i to k; OZ_i presents the orientation differences within the region of minutiae i, α_i denotes the angle between the orientation of minutiae i with the direction of the interior angle bisector of corner i. The pixels in the square centered around minutiae i within the radius r (r is an empirical parameter r = 15 in our algorithm) are forming the region of the minutiae i. OZ_i is computed as follows:

$$OZ_i = \frac{\sum_{i=x0r}^{i=x0+r} \sum_{j=y0r}^{j=y0+r} |\text{Ori}(i,j) - \text{Ori}(x0, y0)|}{2r \bullet 2r} \quad (1)$$

where r is the radius of region, and Ori(i, j) is the orientation at image point (i,j).

The meaning of the parameters $\{d_{ik}, d_{jk}, \psi_j, \psi_k, OZ_j, OZ_k, \alpha_j, \alpha_k\}$ is similar to $\{d_{ij}, \psi_i, OZ_i, \alpha_i\}$. It is clear that the local triangle structure feature vector FT_k is independent from the rotation and translation of the fingerprint. Fig. 2 shows a local triangle structure of the fingerprint.

An exhaustive search will be done to construct the triangles as no prior minutiae correspondence is established. The triangles are constructed by the triplets of minutiae satisfy the following constraint; it means that a minutia belongs to many triangles formed with other minutiae. There is one constraint during the process of constructing the local triangles: the maximum length of the edge in triangle should be less than thr_1, and the minimum length of the edge should be greater than thr_2. As the fingerprint is deformed, the distance between two minutiae (vertexes of the triangle) should not be long. The large deformation is formed by the accumulation from all of the regions between minutiae [11]. thr_1 and thr_2 are empirical parameters (set different value for different database $thr_1 = 150$ pixels, $thr_2 = 10$ pixels for FVC2004 DB1 in the proposed algorithm).
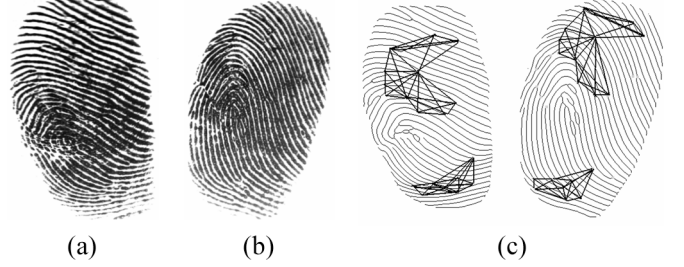
Then, the feature vector set $F = \{FT_1, FT_2, \cdots, FT_N\}$, which consists of feature vectors $FT_k, k = 1, 2, \ldots$ N, of all local triangles detected from a fingerprint, is used to represent the image. Fingerprint matching is to find a similarity between two feature vector set, one from the template and another from the input fingerprint, respectively.

B. Learning Genuine Distorted Pattern Parameters Space

Before measuring the similarity between the fuzzy feature set, we define the genuine distorted pattern parameter space, which is derived from a set of genuine matching attempts.

Suppose $FT_{Tk} = \{d_{ij}, d_{ik}, d_{jk}, \psi_i, \psi_j, \psi_k, OZ_i, OZ_j, OZ_k, \alpha_i, \alpha_j, \alpha_k\}$ is a local triangle feature in a template fingerprint and $FT_{Ik} = \{d'_{ij}, d'_{ik}, d'_{jk}, \psi'_i, \psi'_j, \psi'_k, OZ'_i, OZ'_j, OZ'_k, \alpha'_i, \alpha'_j, \alpha'_k\}$ is a local triangle feature in an input fingerprint. Four distorted pattern parameters, vectors $\vec{len}_{\text{diff}}, \vec{\psi}_{\text{diff}}, \vec{OZ}_{\text{diff}}$, and $\vec{\alpha}_{\text{diff}}$ are calculated as follows:

$$\vec{len}_{\text{diff}} = \{|d_{ij} - d'_{ij}|, |d_{ik} - d'_{ik}|, |d_{jk} - d'_{jk}|\} \quad (2)$$

$$\vec{\psi}_{\text{diff}} = \{|\psi_{ij} - \psi'_{ij}|, |\psi_{ik} - \psi'_{ik}|, |\psi_{jk} - \psi'_{jk}|\} \quad (3)$$

$$\vec{OZ}_{\text{diff}} = \{|OZ_i - OZ'_i|, |OZ_j - OZ'_j|, |OZ_k - OZ'_k|\} \quad (4)$$

$$\vec{\alpha}_{\text{diff}} = \{|\alpha_i - \alpha'_i|, |\alpha_j - \alpha'_j|, |\alpha_k - \alpha'_k|\}. \quad (5)$$

These distorted pattern parameters construct the deformed pattern feature vector $\vec{f}(\vec{len}_{\text{diff}}, \vec{\psi}_{\text{diff}}, \vec{OZ}_{\text{diff}}, \vec{\alpha}_{\text{diff}})$. To learn the genuine distorted pattern parameter, we applied a set of distorted fingerprint images to derive a genuine distorted pattern parameter space. In order to ensure the samples are representative of various types of distortions, we choose the corresponding training samples for each database. For example, in the FVC2004 databases [3], we used training set B to derive the genuine distorted pattern parameter space for benchmark set A.

Fig. 3 shows a genuine distorted pattern derived from two images in FVC2004 DB1 Set B. In this database, the distortion between some impressions from the same finger is large as shown in Fig. 1. The database set B contains 80 fingerprint images captured from ten different fingers, eight images for each finger. The image was acquired through the "CrossMatch V300" optical sensor. The size of the image is 640*480 pixels with the resolution being about 500 dpi. In order to compute the genuine distorted pattern parameter space of FVC2004 DB1, we matched those impressions from the same finger and trained the distorted pattern parameters in Set B.

C. FFM

Based upon fuzzy feature representation of fingerprints, the similarity between the fuzzy feature is used to characterize the similarity between fingerprints. We introduce a fuzzy similarity measure for two triangles and extend it to construct a similarity vector including the triangle-level similarity for all triangles in two fingerprints. Accordingly, a similarity vector pair is defined to illustrate the resemblance between two images. The FFM method maps a similarity vector pair to a normalized quantity, within the real interval [0, 1], which quantifies the overall image to image similarity.

1) Fuzzy Similarity Between Triangles: All elements in the genuine distorted pattern parameter space construct the fuzzy feature set $\widetilde{G}$. The center $(\widetilde{g})$ of the fuzzy feature set $\widetilde{G}$ is used to represent feature set $\widetilde{G}$, with $\widetilde{g}$ defined as

$$\widetilde{g} = \frac{\sum_{\vec{f} \in \widetilde{G}} \vec{f}}{V(\widetilde{G})} \tag{6}$$

where $\vec{f}$ represents a feature vector in $\widetilde{G}$, $V(\widetilde{G})$ denotes the volume of $\widetilde{G}$, which is essentially the mean of all elements of the feature set, and it may not be an element of the feature set. While averaging over all features in a feature set increases the robustness of the fuzzy feature, at the same time, lots of useful information are submerged into the smoothing process because a set of feature vectors is mapped to a single feature vector. Here, we chose only the first-order moment to describe the fuzzy feature set, and the experimental results prove that it is simple and efficient for using the center $(\widetilde{g})$ to represent feature set $\widetilde{G}$.

Suppose $FT_{Tk} = \{d_{ij}, d_{ik}, d_{jk}, \psi_i, \psi_j, \psi_k, OZ_i, OZ_j, OZ_k, \alpha_i, \alpha_j, \alpha_k\}$ is a local triangle in the template fingerprint and $FT_{Ik} = \{d'_{ij}, d'_{ik}, d'_{jk}, \psi'_i, \psi'_j, \psi'_k, OZ'_i, OZ'_j, OZ'_k, \alpha'_i, \alpha'_j, \alpha'_k\}$ is a local triangle in the input fingerprint, the following method is employed to measure the similarity between FT_{Tk} and FT_{Ik}. First, calculate the deformed pattern feature vector $\vec{f}_k$ ($len_{diff}, \vec{\psi}_{diff}, \vec{OZ}_{diff}, \vec{\alpha}_{diff}$); then measure the degree of membership of $\vec{f}_k$ to the fuzzy feature set $\widetilde{G}$.

Building or choosing a proper membership function is application dependent. The most commonly used prototype membership functions are cone, exponential, and Cauchy functions [19]. In our algorithm, the modified Cauchy function is chosen due to its good expressiveness and high-computational efficiency [20].

The membership function of $\vec{f}$ to fuzzy feature set $\widetilde{G} : C(\vec{f}) \rightarrow [0, 1]$, is defined as

$$C(\vec{f}) = \begin{cases} 1, & \text{if } h(\vec{f}, \vec{g}) = \text{True} \\ \frac{1}{1 + \left(\frac{\|\vec{f} - \vec{g}\|}{m}\right)^a}, & \text{otherwise} \end{cases} \tag{7}$$

where $\vec{f} \in \widetilde{G}$, m and $a \in \Re$, $m > 0$, $a >= 0$. If and only if the value of each entry in feature vector $\vec{f}$ is less than the value of corresponding entry in feature vector $\widetilde{g}$, $h(\vec{f}, \vec{g}) = \text{True}$. $\widetilde{g}$ is the center location of the fuzzy set, m represents the width ($\|\vec{f} - \vec{g}\|$ for $C(\vec{f}) = 0.5$) of the function, and a determines the smoothness of the function. Generally, m and a describe the grade of fuzziness of the corresponding feature. For fixed m, the grade of fuzziness increases while a decreases. For fixed a, the grade of fuzziness increases as m increases. It is clear that the farther a feature vector moves away from the cluster center, the lower the degree of membership to the fuzzy feature is.

2) Fuzzy Feature Matching: Similarity Between Fingerprints: It is clear that the image-level similarity is constructed from triangle-level similarities. Let $T = \{\vec{FT}_t : 1 \leq t \leq u, u$ be the number of all triangles detected from the template fingerprint, $\}$ represents the template fingerprint, and $I = \vec{FT}_i : 1 \leq i \leq v, v$ is the number of all triangles detected from the input fingerprint, $\}$ represents the input fingerprint. First, for every $\vec{FT}_t \in T$, we define the similarity measure for it and I as

$$l_t^I = \max\left\{ C(\vec{FT}_t - \vec{FT}_i) | i = 1 \ldots v. \right\} \tag{8}$$

Combining l_t^I together, we get a vector

$$\vec{l}^I = \left[l_1^I, l_2^I, \cdots, l_u^I \right]^T. \tag{9}$$

Likewise, for every $\vec{FT}_i \in I$, we define the similarity measure for it and T as

$$l_i^T = \max\left\{ C(\vec{FT}_i - \vec{FT}_t) | t = 1 \ldots u \right\}. \tag{10}$$

Combining l_i^T together, we get a vector

$$\vec{l}^T = \left[l_1^T, l_2^T, \cdots, l_v^T \right]^T. \tag{11}$$

It is clear that $\vec{l}^I$ describes the similarity between the individual fuzzy feature in T and all of the fuzzy features in I, and $\vec{l}^T$ illustrates the similarity between individual fuzzy features in I and all fuzzy features in T. Thus, we define a similarity vector for T and I, denoted by $\vec{L}^{(T,I)}$, as $\vec{L}^{(T,I)} = \begin{bmatrix} \vec{l}^I \\ \vec{l}^T \end{bmatrix}$, which is a $(u + v)$ dimensional vector with values of all entries within the real interval [0,1].

The FFM method is applied to provide an overall image to image similarity by summation of all the weighted entries of similarity vectors $\vec{L}^{(T,I)}$. The FFM method computes the inner products of similarity vectors $\vec{L}^{(T,I)}$ with weight vectors w. There are many options to choose weight vectors w. We can take the location of the triangles into account and assign higher weights to triangles closer to the center of the fingerprint (center-favored scheme, assuming the triangles near the image center are more reliable). Another choice is the area scheme. It takes the area covered by the triangle as the weight based on the viewpoint that the triangle of the proper area in a fingerprint is more reliable. In the FFM method, both area- and center-favored schemes are used. The weight vectors w are defined as

$$\vec{w} = (1 - p)\vec{w}_A + p\vec{w}_B \tag{12}$$

$$\vec{w}_A = \begin{bmatrix} \vec{w}_A^I \\ \vec{w}_A^I \end{bmatrix} = \begin{bmatrix} w_{A_1} \\ \vdots \\ w_{A_{u+v}} \end{bmatrix}, w_{A_i} = \frac{1}{S_A} e^{-\frac{(S_i - S_p)^2}{\delta}},$$

$$S_A = \sum_{i=1}^{u+v} e^{-\frac{(S_i - S_p)^2}{\delta}} \tag{13}$$

INPUT: the minutiae number n, m of the template and query fingerprints;

OUTPUT: s_t, the number of matched triangles between the template and input fingerprints;

1) For $i = 1$ to n;

2) Generate each minutiae details (position, minutiae orientation, orientation differences within the region) for template;

3) Next i

4) For $i = 1$ to m;

5) Generate each minutiae details (position, minutiae orientation, orientation differences within the region) for query;

6) Next i

7) For $i = 1$ to n; For $j = i+1$ to n; For $k = j+1$ to n;

8) Compute each local triangle feature details ($d_{ij}, d_{ik}, d_{jk}, \psi_i, \psi_j, \psi_k, oz_i, oz_j, oz_k, \alpha_i, \alpha_j, \alpha_k$) for template;

9) Next k; Next j; Next i

10) Suppose a triangles have been constructed for the template fingerprint

11) For $i = 1$ to m; For $j = i+1$ to m; For $k = j+1$ to m;

12) Compute each local triangle feature details ($d_{pq}, d_{pr}, d_{qr}, \psi_p, \psi_q, \psi_r, oz_p, oz_q, oz_r, \alpha_p, \alpha_q, \alpha_r$) for query;

13) Next k; Next j; Next i

14) Suppose b triangles have been constructed for the query fingerprint

15) For $ii = 1$ to a; For $jj = 1$ to b

16) If ($\left| d_{ij} - d_{pq} \right| < thr_d \; and \; \left| d_{ik} - d_{pr} \right| < thr_d \; and \; \left| d_{jk} - d_{qr} \right| < thr_d$

and $\left| \psi_i - \psi_p \right| < thr_\psi \; and \; \left| \psi_j - \psi_q \right| < thr_\psi \; and \; \left| \psi_k - \psi_r \right| < thr_\psi$

and $\left| oz_i - oz_p \right| < thr_{oz} \; and \; \left| oz_j - oz_q \right| < thr_{oz} \; and \; \left| oz_k - oz_r \right| < thr_{oz}$

and $\left| \alpha_i - \alpha_p \right| < thr_\alpha \; and \; \left| \alpha_j - \alpha_q \right| < thr_\alpha \; and \; \left| \alpha_k - \alpha_r \right| < thr_\alpha$)

17) $s_t = s_t + 1$;

18) End if;

19) Next jj; Next ii

Fig. 4. Basic simulation procedure.

$$\overrightarrow{w_B} = \begin{bmatrix} \overrightarrow{w_B^I} \\ \overrightarrow{w_B^T} \end{bmatrix} = \begin{bmatrix} w_{B_1} \\ \vdots \\ w_{B_{u+v}} \end{bmatrix}, w_B = \frac{1}{S_B} e^{-\|r_i - R\|},$$

$$S_B = \sum_{i=1}^{u+v} e^{-\|r_i - R\|}, R = \begin{cases} R_T & i = 1 \dots u \\ R_I & i = u \dots u + v \end{cases} \quad (14)$$

where S_p is the desired area of the triangle, R_T is the center of template image, R_I is the center of the input image, r_i is the barycenter of the ith triangle. $\vec{w}_A$ contains the normalized area percentage of both template and input fingerprints, $\vec{w}_B$ contains normalized weights which favor triangles near the image center, $p \in [0, 1]$ adjusts the significance of $\vec{w}_A$ and $\vec{w}_B$. Consequently, the FFM measure for template and input fingerprints is defined as

$$\text{Sim} = [(1 - p)\vec{w}_A + p\vec{w}_B] \, \vec{L}^{(T,I)}. \quad (15)$$

IV. PERFORMANCE ANALYSIS

The important works were presented by Pankanti *et al.* [21] and Tan *et al.* [22], which measure the details to establish the correspondence between two fingerprints. Different from Pankanti's model, Tan not only assumes that the uncertainty area of any two minutiae may overlap each other, but also measure the relationship between different minutiae. They make the following assumptions to estimate the probability: 1) do not distinguish endpoint and bifurcation but take both of them as the point feature; 2) point features are distributed uniformly in the fingerprints, however, the uncertainty area of different minutiae may overlap; 3) correspondence of a minutiae pair is independent and each correspondence is equally important; 4) fingerprint quality is not explicitly taken into account in the model; and 5) the template and query fingerprints are well aligned.

We analyze our work based on Tan's model. Different from his assumptions, there is no need to align the template and query fingerprints because the local triangle structure feature we are using is independent from the rotation and translation of the fingerprint.

A. Performance Analysis of FFM Based on the Local Triangle Feature Set

In our algorithm, the fingerprint is represented by the local triangle feature set. The similarity between template and input fingerprints is constructed by triangle similarities. It is difficult to get the closed-form equation for $P(Sim > thre/M = m, N = n)$, where M, N are the minutiae number of the template and input fingerprints, respectively, $P\{\bullet\}$ is the probability that the similarity between the template and input fingerprints is greater than threshold $thre$. Here, we will analyze $P_M, N(M3 = s)$, where $M3$ is the matched number of triplets of minutiae which satisfy all of the criterion in the matching process, and $P_{M,N(.)}$ is the probability of the local triangle feature set matching model.

Suppose 1) the number of all triangles detected from the template and input fingerprints are $\boldsymbol{u}$ and $\boldsymbol{v}$, respectively; 2) only consider the entry that triangle similarity is equal to 1 in the similarity vector $\vec{L}^{(T,I)}$, and 3) choosing the simplest weight vectors $w = (1/\boldsymbol{u} + \boldsymbol{v}) \cdot \boldsymbol{I}$, I is the unit vector.

Since for each triangle, the feature is represented by vector $\{d_{ij}, d_{ik}, d_{jk}, \psi_i, \psi_j, \psi_k, OZ_i, OZ_j, OZ_k, \alpha_i, \alpha_j, \alpha_k\}$ and those entries of the vector are not independent, they may have an effect on other entries. It is difficult to get the closed-form equation for $P_{M,N}(M_3 = s)$. We use a statistical method to estimate $P_{M,N}(M_3 = s)$ and its 95% confidence interval $\bar{P}_{M,N,Con=95\%}(M_3 = s)$. Then, we can calculate the expectation of the probability distribution function (PDF) of the local triangle feature set matching model as $E_{Con=95\%}(M_3 = s)$.

B. Estimation of $P_{M,N}(M_3 = s)$

Our estimation parameters include $thr_d = 15$ pixels, $thr_\psi = 15^0$, $thr_\alpha = 15^0$, $thr_{oz} = 5^0$. It is an expensive computation to search all possible situations to find $P_{M,N}(M_3 = s)$. Therefore, we use simulations to estimate its mean and 95% confidence interval. The basic simulation procedure is shown in Fig. 4. We performed the tests 100 times, and each test was composed of 10^8 times simulation (i.e., we repeated the basic simulation procedure $100 * 10^8$ times). Fig. 5 shows the detail of $P_{M,N}(M_3 = s)$ for different values of $M3$ with their 95% confidence interval under $M = 36$ and $N = 36$. We observed that the 95% confidence interval of the estimated distribution was very small, the maximum length of the 95% confidence interval in Fig. 5 was 5.6×10^{-4}. Obviously, the results of the 100 tests are very consistent. Table I indicates the error rates for different M, N, and s. We find that the average number of template triangles is almost equal to the average number of input triangles as the minutiae number for the template and input fingerprints is the same. In addition, we also find that if all of the other parameters are fixed, the smaller the number of minutiae in the template and query fingerprints, the lower the probability that they are similar for the same $\boldsymbol{s}$.
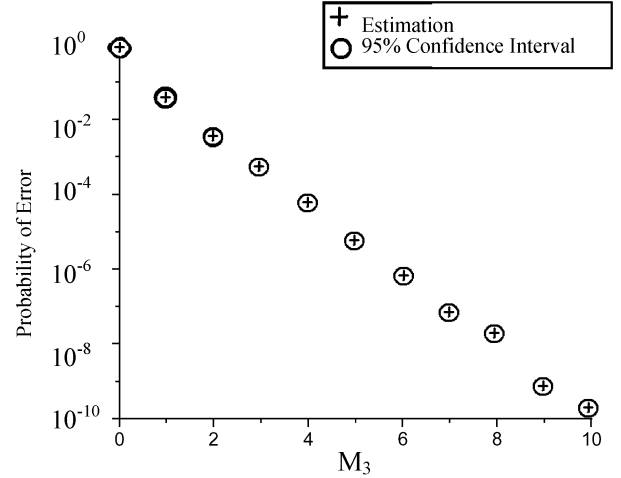

Fig. 5. Simulation results of $P_{M=36,N=36}(M_3 = s)$ and their 95% confidence intervals.

TABLE I
ESTIMATED ERROR RATE FOR DIFFERENT M, N, AND $\boldsymbol{s}$, * REPRESENT THAT NONE OF THE CASES HAVE OCCURRED UNDER THESE CONDITIONS. $\boldsymbol{u}$ AND $\boldsymbol{v}$ ARE THE NUMBER OF ALL TRIANGLES DETECTED FROM THE TEMPLATE AND INPUT FINGERPRINTS, RESPECTIVELY

M	N	Average value of $\boldsymbol{u}$	Average value of $\boldsymbol{v}$	$P_{M,N}(M_3 = s)$					
				8	10	12	15	20	25
60	60	3732	3731	2.3×10^{-3}	6.3×10^{-4}	1.6×10^{-4}	1.8×10^{-5}	6.7×10^{-7}	6.7×10^{-8}
45	45	2151	2152	1.1×10^{-5}	7.8×10^{-7}	1.1×10^{-8}	2.1×10^{-9}	*	*
36	36	1078	1079	5.6×10^{-8}	6.5×10^{-9}	8.3×10^{-10}	*	*	*
20	20	292	292	1.5×10^{-10}	*	*	*	*	*

V. EXPERIMENTAL RESULTS

The proposed algorithm has been evaluated on the fingerprints database of NIST 24 [23] and FVC2004. The fingerprints in NIST 24 have significant plastic distortions and can be used to determine how well the system tolerates significant plastic distortions. In FVC2004, databases are more difficult than FVC2000/FVC2002. In FVC2004, emphasis is on distortion, and dry and wet fingerprints. Especially in DB1 and DB3 of FVC2004, the distortion between some fingerprints from the same finger is large.

Our algorithm is compared with the methods described by Luo et al. [8] and Bazen et al. [1]. We also perform comparisons with other FVC2004 participants' algorithms.

A. Performance on NIST 24

NIST Special Database 24 [23] contains Moving Picture Experts Group (MPEG-2) compressed digital video of live-scan fingerprint data. The database is distributed for developing and testing the fingerprint verification systems. There are two parts: the first contains 10 s (300 frames, 720×480 pixels) of fingerprint data with plastic distortions, and the second contains 10 s of fingerprints at various rotated angles. The database includes 10 samples (five male and five female) of all ten fingers, for a
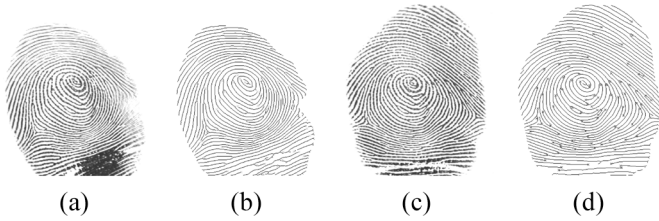
(a)   (b)   (c)   (d)

Fig. 6. Experimental results on two fingerprints in NIST 24. The images have been scaled for view: (a) original image. (b) thinned image of (a). (c) original image, and (d) enhanced image of (c). The similarity of these two fingerprints is 0. 62272.

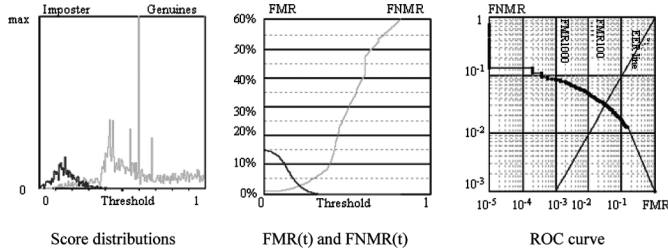Score distributions   FMR(t) and FNMR(t)   ROC curve

Fig. 7. Experimental results of our algorithm on NIST 24. The tested database contains 1000 fingerprint images. Ten individual frames were extracted for every MPEG-2 video file in NIST 24.

(a)   (b)   (c)   (d)

Fig. 8. Experimental results of the proposed algorithm on 109_3.tif and 109_4.tif in FVC2004 DB1. The images have been cropped and scaled for view. (a) 109_3.tif, (b) enhanced image of 109_3, (c)109_4.tif, (d) the thinned image of 109_4. The similarity of these two fingerprints is 0.523 00.
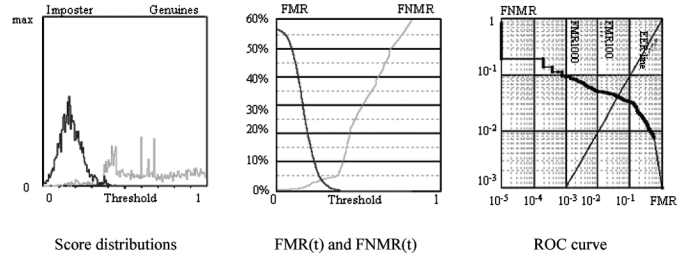

Score distributions   FMR(t) and FNMR(t)   ROC curve

Fig. 9. Experimental results of our algorithm on FVC2004 DB1_A. The fingerprint images were acquired through an optical sensor.

total of 100 MPEG-2 video files. The MPEG-2 files can also be decoded into individual frames and used to test minutiae-based verifications and determine how well the system tolerates significant plastic distortions.

We extract a set of images from NIST Special DB 24 to evaluate how well the proposed algorithms tolerate the significant plastic distortions. For every MPEG-2 video file in NIST 24, ten individual frames were extracted. Hence, the tested database contains $1000\,(100*10)$ fingerprint images. Our algorithm is evaluated according to FVC rules. Each sample is matched against the remaining samples of the same finger in genuine match. The total number of genuine tests (in case no enrollment rejections occur) is $((10*9)/2)*100 = 4,500$. In an imposter match, the first sample of each finger is matched against the first sample of the remaining fingers. Hence, the total number of false acceptance tests (in case no enrollment rejections occur) is $((100*99)/2) = 4,950$. In this database, the average number of minutiae is 75, and the average number of triangles detected from the fingerprints is 6652.

Fig. 6 shows a fingerprint pair with large distortion from NIST 24, (a) and (c) are the original images, (b) and (d) indicate the thinned results of (a) and (c), respectively. Using the proposed algorithm, the similarity between these two fingerprints is 0.622 72. The performance of our algorithm on NIST 24 is shown in Fig. 7, the EER is 3.11%. The average time for matching two minutiae sets is 1.21 s on an AMD Athlon 1600+ (1.41 GHz) PC.

B. Performance on FVC2004 DB1

The fingerprints of FVC2004 DB1 were acquired through optical sensor "CrossMatch V300." The database set A contains 800 images captured from 100 different fingers, eight images for each finger. Fig. 1 shows an example of large distortion from FVC2004 DB1 (102_3.tif and 102_5.tif). Using our algo-

rithm, the similarity between these two fingerprints is 0.430 12. Fig. 8 shows another fingerprint pair with large distortion from FVC2004 DB1. The similarity between these two fingerprints is 0.523 00. In this database, the average number of minutiae is 43, and the average number of triangles is 2613.

The algorithm performance on FVC2004 DB1 is shown in Fig. 9. From Fig. 9, we find that the similarity threshold at the EER point is about 0.265, so we judge that those two fingerprint pairs come from the same finger. The EER of the proposed algorithm on FVC2004 DB1 is 4.06%. The average time for matching two minutiae sets is 1.12 s on an AMD Athlon 1600+ (1.41 GHz) PC.

C. Performance on FVC2004 DB3

The fingerprints of FVC2004 DB3 were acquired through the thermal sweeping sensor "FingerChip FCD4B14CB" by Atmel. The size of the image is $300*480$ pixels with a resolution of 512 dpi. In this database, the distortion between some fingerprints from the same finger is large. Fig. 10 shows a fingerprint pair with large distortion from FVC2004 DB3. The similarity between these two fingerprints is 0.562 35 by our algorithm. In this database, the average number of minutiae is 56, and the average number of triangles is 3668.

The performance of the proposed algorithm on FVC2004 DB3 is indicated in Fig. 11. The similarity threshold at the EER point is about 0.255, so we judge that this pair comes from the same finger. The EER of the proposed algorithm on FVC2004 DB3 is 1.35%. The average time for matching two minutiae sets is 1.08 s on the AMD Athlon 1600+ (1.41 GHz) PC.

D. Comparison of FFM with Other Algorithms

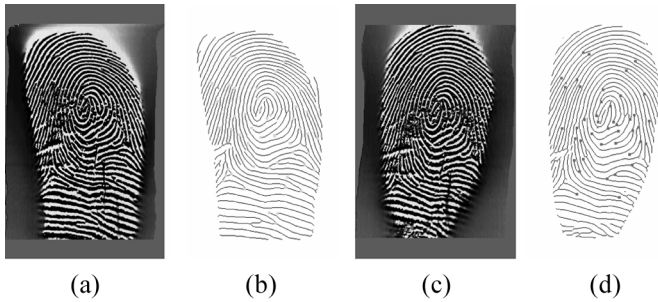The bounding box and the TPS model are two traditional methods in dealing with nonlinear distortions. The proposed al-

Fig. 10. Experimental results of the proposed algorithm on 103_2.tif and 103_4.tif in FVC2004 DB3. The images have been scaled for view. (a) 103_2.tif, (b) enhanced image of 103_2, (c) 103_4.tif, (d) enhanced image of 103_4. The similarity of these two fingerprints is 0.56235.
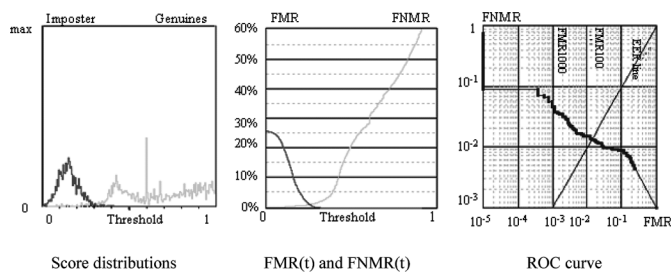

Fig. 11. Experimental results of our algorithm on FVC2004 DB3_A. The fingerprint images were acquired through the thermal sweeping sensor.

gorithm is compared with these two methods, Luo's algorithm [8] (bounding box) and Bazen's algorithm [1] (TPS model). The comparisons are performed with other FVC2004 participants' algorithms as well.

The comparison of our algorithm with Luo's [8] is carried out on FVC2004 DB1. In Luo's method, a changeable bounding box has been used during the matching process. It is robust to nonlinear deformations. However, the distortion in some impressions from the same finger captured from the CrossMatch sensor is large. In order to tolerate the apart matching minutiae pairs caused by distortion, the size of the bounding boxes has to be increased. However, as a side effect, it gives nonmatching minutiae pairs a higher probability to get matched, resulting in a higher FAR. Table II lists the comparison of the matching score of our algorithm to Luo's method. It is clear that case 1 and case 2 have been successfully matched in our FFM algorithm. While for Luo's method, when the size of the bounding boxes is 15, case 1 and case 2 are false rejected; and when size of the bounding boxes is increased to 25, case 2 is accepted but case 1 is false rejected; meanwhile, EER is increased from 9.13% to 9.92% (the size of the bounding boxes is obtained according to the experiments). Moreover, the EER of our algorithm is 4.06%, which is much lower than Luo's method of 9.13%.

Our algorithm contrasts with Bazen's algorithm [1] as well. In their training database of FVC2002 DB1, the EER turned out to be 1.8% with $r0 = 5$ for elastic matching. While in our algorithm, the EER on FVC2002 DB1 is only 0.26%. Our experimental results on FVC2002 DB1 are shown in Fig. 12. The results confirm that the performance of our algorithm exceeds Bazen's algorithm.

TABLE II
COMPARISON OF MATCHING SCORE IN THE FFM ALGORITHM TO LUO'S METHOD [8]

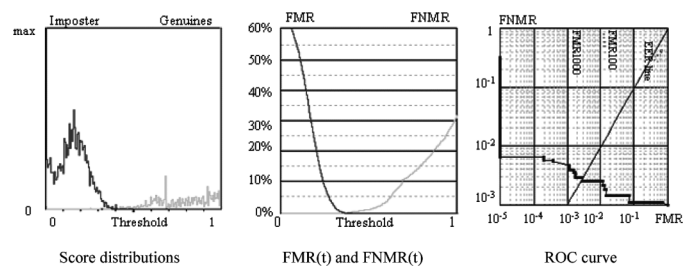| Performance comparison	The proposed algorithm	Luo's method: size of the bounding boxes = 15	Luo's method: size of the bounding boxes = 25
Score of case 1 in figure 1	0.43012	0.050000	0.194000
Score of case 2 in figure 8	0.52300	0.061800	0.273600
Score threshold at EER point	0. 26100	0.152000	0.213100
EER(on FVC2004 DB1_A)	4.06%	9.13%	9.92%

Fig. 12. Experimental results of the proposed algorithm on FVC2002 DB1.

TABLE III
AVERAGE PERFORMANCE COMPARISON OF OUR ALGORITHM WITH OTHER FVC2004 PARTICIPANTS' ALGORITHMS OVER THE FOUR DATABASES

Algorithm	Avg EER	Avg FMR 100	Avg FMR 1000	Avg Zero FMR
P101	2.07%	2.54%	4.70%	6.21%
P047	2.10%	2.96%	4.61%	6.59%
P071	2.30%	2.73%	5.10%	10.01%
P004	2.45%	3.27%	5.63%	7.34%
P039	2.90%	4.57%	7.44%	32.13%
The proposed algorithm	2.05%	2.46%	5.05%	8.03%

The comparisons are also done with other FVC2004 participants' algorithms. Table III lists the average performance of our algorithm with other FVC2004 algorithms over the four databases. The detailed performances of FVC2004 algorithms can be seen from the website http://bias.csr.unibo.it/fvc2004/. The proposed algorithm demonstrates excellent results and it is even better than our previously developed algorithm [16]. (In FVC2004, the algorithm of P071 was designed by our lab.)

VI. CONCLUSION AND DISCUSSION

Coping with nonlinear distortions in fingerprint matching is a challenging task. We proposed a novel method for deformed fingerprints matching. The fingerprint is represented by the fuzzy feature: local triangle feature set. The similarity between the fuzzy feature is used to character the similarity between fingerprints. We introduce a fuzzy similarity measurement for two triangles and extend it to construct a similarity vector including the triangle-level similarity in two fingerprints. Accordingly, a

similarity vector pair is defined to illustrate the resemblance between two fingerprints. Finally, the FFM method maps a similarity vector pair to a normalized quantity which quantifies the overall image to image similarity within the real interval [0, 1]. The proposed algorithm has been evaluated with NIST 24 and FVC2004 fingerprint databases. Experimental results confirm that our algorithm works well with the nonlinear distortions. The EER of the proposed algorithm on NIST 24 is 3.11%. In the fingerprints database, DB1 and DB3 of FVC2004, EER are 4.06% and 1.35%, respectively, although there are large distortions between some fingerprints from the same finger. In addition, our algorithm is good at processing time, the average time for matching two minutiae sets is about 1.1 s. However, there is a drawback for our algorithm. For the genuine match, the overlapping area between the template and input fingerprint should be large. Further research is continuing to improve the algorithm.

ACKNOWLEDGMENT

REFERENCES

[1] A. M. Bazen and S. H. Gerez, "Fingerprint matching by thin-plate spline modeling of elastic deformations," *Pattern Recognit.*, vol. 36, no. 8, pp. 1859–1867, 2003.

[2] A. Ross, S. Dass, and A. K. Jain, "A deformable model for fingerprint matching," *Pattern Recognit.*, vol. 38, no. 1, pp. 95–103, Jan. 2005.

[3] Biometric Systems Lab, Pattern Recognition and Image Processing Lab. Biometric Test Center [Online]. Available: http://bias.csr.unibo.it/fvc2004/, 2004

[4] N. K. Ratha and R. M. Bolle, "Effect of controlled acquisition on fingerprint matching," in *Proc. 14th ICPR*, 1998, vol. 2, pp. 1659–1661.

[5] C. Dorai, N. Ratha, and R. Bolle, "Detecting dynamic behavior in compressed fingerprint videos: distortion," in *Proc. CVPR*, Hilton Head, SC., Jun. 2000, pp. 2320–2326.

[6] H. Chen, J. Tian, and X. Yan, "Fingerprint matching with registration pattern inspection," Proc. AVBPA, Lecture Notes Comput. Sci. 2688. New York, Springer, 2003, pp. 327–334.

[7] A. K. Jain, L. Hong, and R. Bolle, "On-line fingerprint verification," *IEEE Trans. Pattern Anal. Mach. Intell.*, vol. 19, no. 4, pp. 302–313, Apr. 1997.

[8] X. P. Luo, J. Tian, and Y. Wu, "A minutia matching algorithm in fingerprint verification," in *Proc. 15th ICPR*, Sep. 2000, vol. 4, pp. 833–836.

[9] D. Lee, K. Choi, and J. Kim, "A robust fingerprint matching algorithm using local alignment," in *Proc. 16th ICPR*, Aug. 2002, vol. 3, pp. 803–806, .

[10] N. Ratha, R. Bolle, V. Pandit, and V. Vaish, "Robust fingerprint authentication using local structural similarity," in *Proc. 5th IEEE Workshop on Applied Computer Vision*, Dec. 2000, vol. 1, pp. 29–34.

[11] Z. M. Kovács-VajnaKovacs-Vajna, "A fingerprint verification system based on triangular matching and dynamic time warping," *IEEE Trans. Pattern Anal. Mach. Intell.*, vol. 22, no. 11, pp. 1266–1276, Nov. 2000.

[12] X. Jiang and W. Y. Yau, "Fingerprint minutiae matching based on the local and global structures," in *Proc. 15th ICPR*, Sep. 2000, vol. 2, pp. 1038–1041.

[13] A. Wahab, S. H. Chin, and E. C. Tan, "Novel approach to automated fingerprint recognition," *Proc. Inst. Elect. Eng., Visual Image Signal Process.*, vol. 145, no. 3, pp. 160–166, Jun. 1998.

[14] R. Cappelli, D. Maio, and D. Maltoni, "Modeling plastic distortion in fingerprint images," in *Proc. ICAPR*, Mar. 2001, pp. 369–376.

[15] A. Senior and R. Bolle, "Improved fingerprint matching by distortion removal," *IEICE Trans. Inf. Syst., Special issue on Biometrics*, vol. E84-D, no. 7, pp. 825–831, Jul. 2001.

[16] X. J. Chen, J. Tian, and X. Yang, "A new algorithm for distorted fingerprints matching based on normalized fuzzy similarity measure," *IEEE Trans. Image Process.*, vol. 15, no. 3, pp. 767–776, Mar. 2006.

[17] L. Hong, Y. Wan, and A. K. Jain, "Fingerprint image enhancement: algorithms and performance evaluation," *IEEE Trans. Pattern Anal. Mach. Intell.*, vol. 20, no. 8, pp. 777–789, Aug. 1998.

[18] X. P. Luo and J. Tian, "Knowledge based fingerprint image enhancement," in *Proc. 15th ICPR*, Sep. 2000, vol. 4, pp. 783–786.

[19] F. Hoppner, F. Klawonn, R. Kruse, and T. Runkler, *Fuzzy Cluster Analysis: Methods For Classification, Data Analysis and Image Recognition*. New York: Wiley, 1999.

[20] Y. X. Chen and J. Z. Wang, "A region-based fuzzy feature match approach to content-based image retrieval," *IEEE Trans. Pattern Anal. Mach. Intell.*, vol. 24, no. 9, pp. 1252–1267, Sep. 2002.

[21] S. Pankanti, S. Prabhakar, and A. K. Jain, "On the individuality of fingerprints," *IEEE Trans. Pattern Anal. Mach. Intell.*, vol. 24, no. 8, pp. 1010–1025, Aug. 2002.

[22] X. J. Tan and B. Bhanu, "On the fundamental performance for fingerprint matching," in *Proc. CVPR*, Jun. 2003, vol. 2, pp. 1063–1069.

[23] NIST Special Database 24 [Online]. Available: http://www.nist.gov/srd/nistsd24.htm.

Xinjian Chen received the B.S. degree in geophysics from Centre South University of Technology, Changsha, China, in 2001, and is currently pursuing the Ph.D. degree from the Center for Biometrics and Security Research, Key Laboratory of Complex Systems and Intelligence Science, Institute of Automation, Chinese Academy of Sciences, Beijing, China.

His research interests include pattern recognition, machine learning, image processing, and their applications in biometrics.
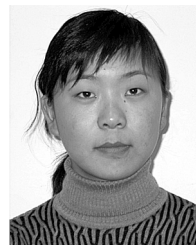
Jie Tian (SM'03) received the Ph.D. degree (Hons.) in artificial intelligence from the Center for Biometrics and Security Research, Key Laboratory of Complex Systems and Intelligence Science Institute of Automation, Chinese Academy of Sciences, Beijing, China, in 1992.

From 1994 to 1996, he was a Postdoctoral Fellow with the Medical Image Processing Group, University of Pennsylvania, Philadelphia. Currently, he is a Professor in the Institute of Automation, Chinese Academy of Sciences. His research interests are pattern recognition, machine learning, image processing, and their applications in biometrics, etc.

Xin Yang received the Ph.D. degree in precision instruments from TianJing University, TianJing, China, in 2000.

Currently, she is a Postdoctoral Fellow with the Institute of Automation, Chinese Academy of Sciences. Her research interests are pattern recognition, and their applications in biometrics, etc.

Yangyang Zhang received the B.S. degrees in electronic engineering and information science from the University of Science and Technology of China, Hefei, in 2001, and is currently pursuing the Ph.D. degree from the Institute of Automation, Chinese Academy of Sciences, Beijing, China.

Her research interests include pattern recognition, machine learning, image processing, and their applications in biometrics.